



## FAILURE ANALYSIS OF A STORAGE PUMP SHAFT

Niculai PASCA, Liviu MARSAVINA, Sebastian MUNTEAN, Radu NEGRU

Affiliation: 1) "Politehnica" University Timisoara, 2) Romanian Academy, Timisoara Branch

Email address: [nicu\\_pasca21@yahoo.com](mailto:nicu_pasca21@yahoo.com)

**Abstract:** The shaft is an important component in hydraulic pumps used to transmit power from electrical motor to the pump impeller. The paper presents failure analysis of a shaft, from a double suction hydraulic pump in operation of approximately 30 years, in a storage station. The shaft material is a Romanian steel, equivalent after their chemical composition and mechanical characteristics with American SAE 4340 steel for which in literature are available necessary data for failure analysis. The paper is structured in two parts: finite element analysis of the pump shaft and an analytical failure analysis for a circumferential crack type, using the failure assessment diagram (FAD). In a modeling program for stress and strain analysis the 3D shaft was loaded in torsion. The numerical results show the maximum stress zones, the stress concentration effect, and the possibility of crack occurrence. For circumferential crack type the failure assessment diagram for Mode III loading were plotted using the stress intensity factor solution. The results indicate the unsafe zone respectively the critical circumferential crack depth, where the shaft cannot operate with defects. This study presents an opportunity related to safe operation condition and remaining life estimation for a storage pump.

**Key words:** finite element analysis, stress, storage pump shaft, failure assessment diagram (FAD)

## 1. INTRODUCTION

Storage pumps all over the world are integrated equipment in hydropower facilities. These pumps are required to allow primarily large flow rate, in addition to operate at high efficiency and tolerant cavitation conditions. In Figure 1 is shown the cross section and the storage pump components: 1 impeller, 2 suction elbow, 3 volute, 4 shaft, 5 radial bearing , 6 radial-axial bearing.

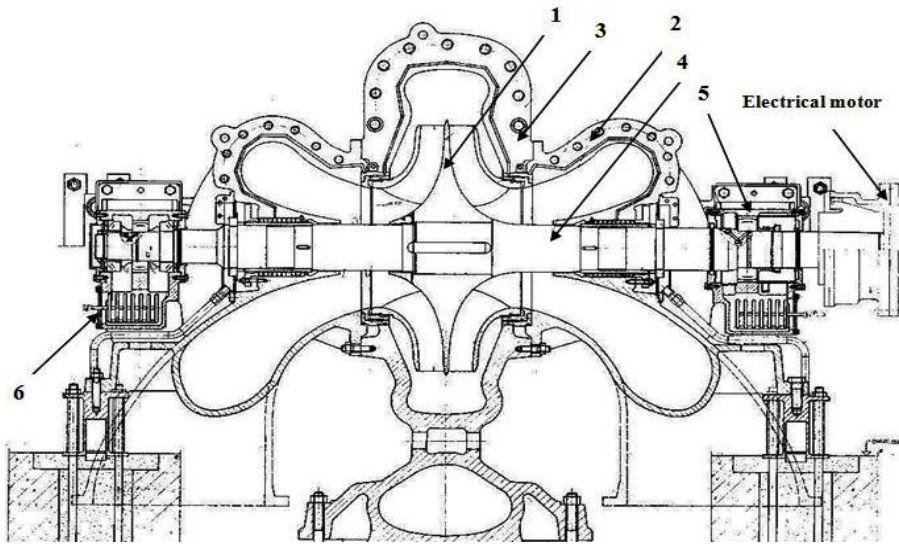


Figure 1. Storage pump cross section.

Table 1: Technical characteristics of the storage pump

Parameters	Symbol	Value
Pumping Head	H [m]	197
Flow rate	Q [m <sup>3</sup> /s]	4
Hydraulic Power	P [kW]	8840
Efficiency	$\eta$ [%]	87.5

The pump shaft fails after approximately 30 years of operating time. In Figures 2 and 3 are presented the shaft fracture surface zone compared with theoretical aspect of a shaft failure in torsion loading condition [1]. This leading to hypotheses that shaft failed in torsion loading condition. In literature other studies present aspects of shaft failure in operating condition [2], [3], and [4]. In [2] the authors present a numerical turbine shaft failure

analysis with a crack propagation analysis using ANSYS and Aflow software. An analysis of the premature failure of two counter shafts used in centrifugal pumps for lifting slurry has been carried out by Das et al. [3]. A collection of pump shaft failures like, corrosion failures on shafts, fatigue failures on shafts and shaft sleeve failures are analyzed [4]. However, these papers have not tackled the failure analysis using failure assessment diagram in mode III.



Figure 2. Fracture surface of the investigated shaft.

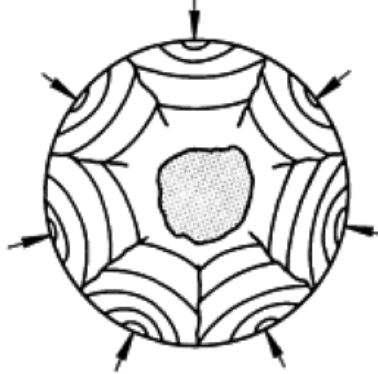


Figure 3. Sketch of fracture surface in torsion loading condition [1].

This paper is structured in five parts which include a problem introduction, the shaft material, a stress and strain numerical analysis, and mode III failure diagram for a circumferential crack in a shaft. The conclusions are drawn in last section.

## 2. STORAGE PUMP SHAFT MATERIAL

The shaft material is a Romanian steel named after STAS 791-66, 34MoCN, with the following chemical composition presented in table 2.

Table 2 Chemical composition and mechanical characteristics according to STAS 791-66 [5] for storage pump shaft material.

Steel name	Chemical composition [%]					
	C	Si	Mn	Cr	Ni	Mo
34 MoCN 15	0.3-0.38	0.17-0.37	0.4-0.7	0.6-1.7	1.4-1.9	0.15-0.3
	Mechanical characteristics					
	Yield Stress $\sigma_y$ [MPa]			Tensile strength $\sigma_r$ [MPa]		
	882.9			1079.1		

Material properties and specially fracture toughness are necessary for failure analysis. Because for the Romanian steel these parameters are not presented in literature, and equivalent steel was searched. In table 3 are presented the material characteristics of the equivalent steel SAE 4340 [5]. It can be observed the chemical composition for both materials are very close.

Table 3 Chemical composition and mechanical characteristics for equivalent steel SAE 4340 [6]

Steel name	Chemical composition [%]					
	C	Si	Mn	Cr	Ni	Mo
SAE 4340	0.37-0.4	0.23	0.7	0.7-0.9	1.83	0.2-0.3
	Mechanical characteristics					
	Yield stress $\sigma_y$ [MPa]			Tensile strength $\sigma_r$ [MPa]		
	834			931		

The fracture toughness for mode III of 4340 steel which is used in failure assessment diagram for mode III construction  $K_{IIIc} = 68.235 \text{ MPa}\sqrt{\text{m}}$  is presented [7].

### 3. STRESS AND STRAIN ANALYSIS

The stress and strain analysis for 3D geometry obtained in modeling software has been performed. The 3D shaft geometry is shown in Figure 4. Using the numerical software ANSYS has been performed a finite element analysis for the shaft.

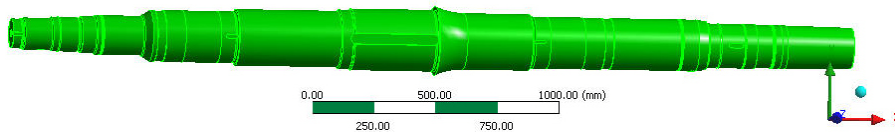


Figure 4. 3D shaft geometry

The shaft model has been meshed using tetrahedral elements type 3D Solid 187, defined by 10 nodes having three degrees of freedom at each node: translations in the nodal x, y, and z directions. The element has plasticity, hyperelasticity, creep, stress stiffening, large deflection, and large strain capabilities. In radial bearing close the electrical motor, where the shaft has an important stress concentrator, a fine mesh was performed, using 2 mm elements size. For this type of mesh the finite elements number was

215045 and 361108 nodes. A detailed stress concentrator zone with mesh refinement is presented in Figure 5.

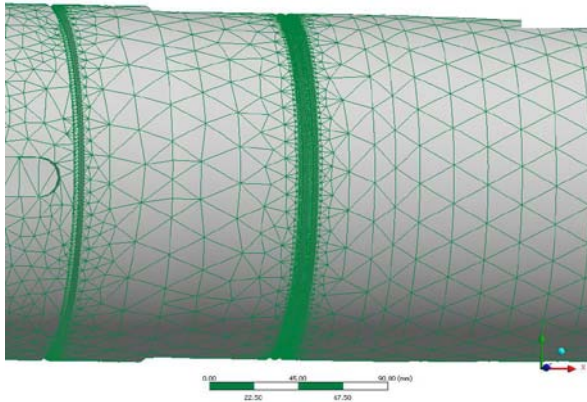


Figure 5. A detailed stress concentrator zone with mesh refinement

The boundary conditions have been made according to real loading form technical data sheets. A torsion loading was imposed from electrical motor which is transmitted to pump impeller located on the shaft middle, marked  $M_t$  torque. Another condition was the impeller weight marked with  $G_r$  and bearings in shaft zones indicate in Figure 6.

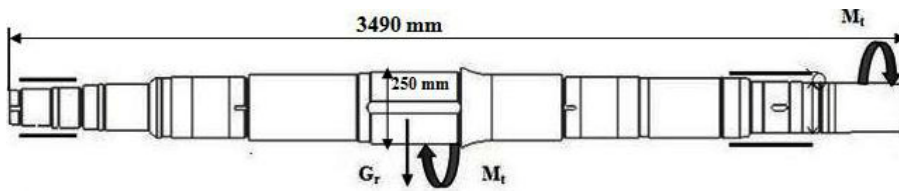


Figure 6. The problem set-up

A convergence study for maximum equivalent stress was performed. For the fine mesh with 428468 elements and 719492 nodes the solutions difference are 0.43% compared with the solution with lower elements and nodes number. In Table 4 are presented the results for 7 meshes with different number of elements and nodes, respectively.

Table 4. Solution convergence study

Simulation case number	Maximum equivalent stress [MPa]	Elements number	Nodes number	Error [%]
1	487.79	215045	361108	
2	487.42	224145	376389	1.46

3	487.32	265452	445752	1.03
4	487.29	304121	510686	0.79
5	487.24	352145	591329	1.11
6	487.22	398456	669096	0.72
7	487.16	428468	719492	0.43

The stress and strain distributions on the pump shaft were obtained using finite element method. As a result, the shear stress ( $\tau_{xy}$ ,  $\tau_{xz}$ ,  $\tau_{yz}$ ), maximum equivalent stress and deformation are presented in figures 7, 8 and 9, respectively.

Results obtained and the fracture surface aspect indicate in Figure 2, show that the fracture occurred in bearing zone after application of shear loading where there is a stress concentrator. The stress results show a maximum in that zone, the maximum equivalent stress as the normal and tangential components is 483.97 MPa. The shear stresses occurring in the concentrator are  $\tau_{xy}$ =131.45 MPa,  $\tau_{yz}$ = 278.78 MPa while  $\tau_{xz}$  is negligible.

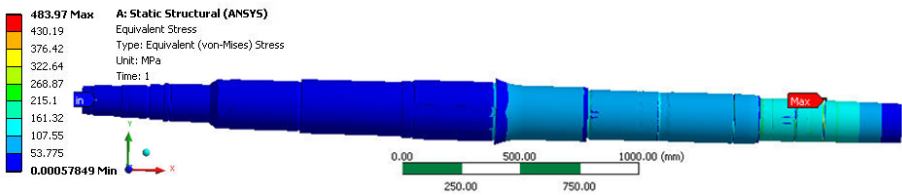


Figure 7. Equivalent stress results on the pump shaft

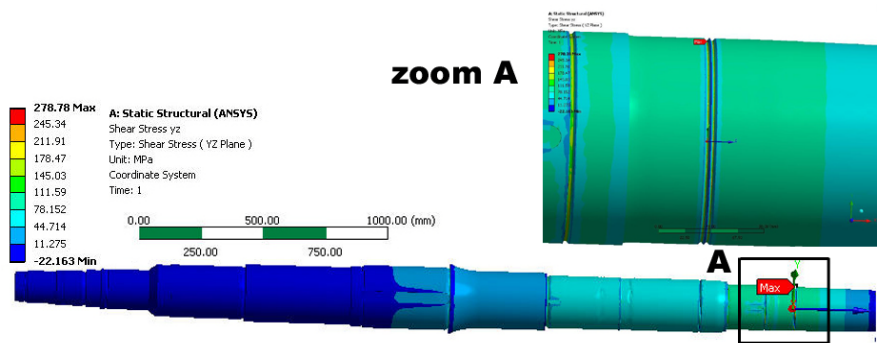


Figure 8. Shear stress results: general view and zoom of the region with maximum value (A region)

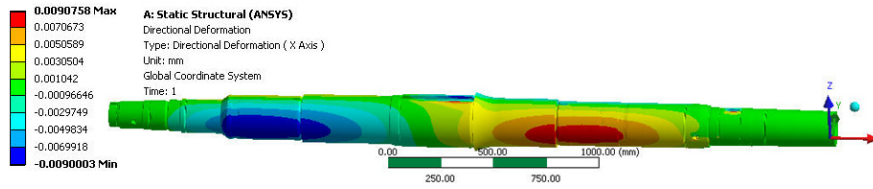


Figure 9. Deformation distribution on the shaft

#### 4. FAILURE ANALYSIS DIAGRAM (FAD)

The failure (or fracture) assessment diagram is an attempt at combining failure criteria based on linear elastic fracture mechanics and plastic collapse. This failure criterion is a function of two parameters  $K_r$  and  $S_r$ , which respectively quantify the elastic fracture component and the plastic collapse component.  $K_r$  and  $S_r$  for failure mode III were calculated using eq. (1). Curve that represents a limit of safe design is plotted in the coordinate system ( $K_r$ ,  $S_r$ ). The safe zone is considerate, the zone below the curve provided  $K_r$  and  $S_r$  in FAD diagram.

$$K_r = \frac{K_{III}}{K_{IIIc}} \quad \text{and} \quad S_r = \frac{\tau}{\tau_c} \quad (1)$$

where  $K_{IIIc}$  [ $\text{MPa m}^{0.5}$ ] is the material fracture toughness in mode III [3] and  $K_{III}$  [ $\text{MPa m}^{0.5}$ ] represents the stress intensity factor in mode III at different crack length calculated with eq. (2):

$$K_{III} = \tau \sqrt{\pi c} F_{III}(a/b) [\text{MPa} \sqrt{m}] \quad \text{and} \quad (2)$$

$$\tau = \frac{2M_t}{\left[ \pi(D - 2c)^3 \right]^{1/2}} [\text{MPa}] \quad (3)$$

where  $F_{III}(a/b)$  is the factor which consider the  $b=D$  shaft diameter 170 mm and  $a$  uncracked zone radius [8],  $c$  crack depth for circumferential crack,  $\tau$  shear stress eq. (3),  $M_t$  torque moment,  $\tau_c$  yield shear stress  $\tau_c = 0.577\tau_y$  [9].

The failure criterion for mode III is presented by 3 models function of plastic zone shape near the crack: Hult-McClintock, Cherepanov and Bilby-Cottrell-Swinden.

$$K_r = \{ 1 - [(S_r)^2 / (1 + B/A)] \}^{1/2} \quad (4)$$

where  $B/A$  is ratio of the semi minor axis to the semi major axis of the elliptic plastic zone.

Eq. (4) is a generalization of this failure criterion, for a customization we have different type of plastic zone near the crack (circle when  $B/A=0$ , elliptic when  $B/A=1$ ). In case of  $B/A=1$ , result Hult-McClintock failure



criterion for mode III. For  $B/A=0$ , eq. (3) results Cherepanov failure criterion. Another failure criterion for mode III, based on the Bilby-Cottrell-Swinden customization has the same form as Dugdale model as eq. (5) [10]:

$$K_r = S_r [(8/\pi^2) \ln \sec(\pi S_r/2)]^{1/2} \quad (5)$$

Based on these failures criterion and the concept presented above were carrying out different shaft circumferential crack depth loaded in mode III.

The failure assessment diagram represented in  $K_r$  and  $S_r$  coordinates and obtained from eq. (1) is presented in Figure 10.

From the failure assessment diagram is observed that for a circumferential crack depth in shaft loaded in mode III, for all 3 failures solution critical depth is 33 mm, after this circumferential crack depth the shaft is in unsafe zone.

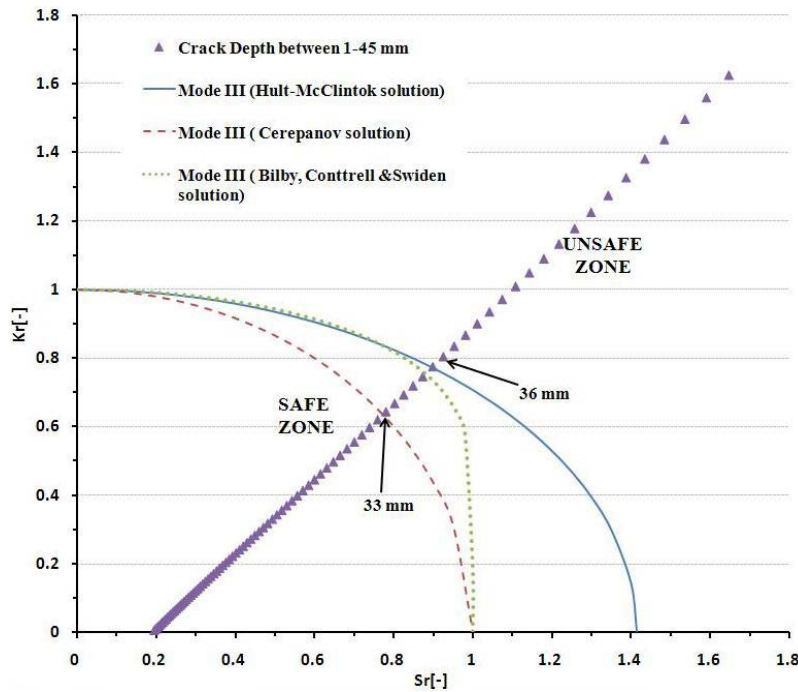


Figure 10. Failure assessment diagram in mode III

For crack depth between 33 mm and 35 mm after Bilby-Cottrell-Swinden and Hult-McClintock failure criterion the shaft is in a safe zone.



## 5. CONCLUSIONS

The paper investigates the failure of the shaft from double suction storage pump using numerical analysis and FAD diagram. The numerical analysis has shown a stress field as well as the deformation distribution. A stress concentration near to the lubrication channel of the bearing is highlighted by shear stress and equivalent stress distribution. The fracture zone aspect indicates a mode III loading produced by torque in order to pass the power from electrical motor to the pump impeller.

The FAD diagram for mode III was developed taking into account three different plastic zone shapes and was applied for circumferential crack. As a result, the three models predict different critical crack depths. However, the value of the maximum crack depth of 33 mm is could be considered the maximum allowable crack depth. The inspection periods could be estimated based on the previous data in order to prevent a catastrophic accident.

## ACKNOWLEDGEMENT

This work was partially supported by the strategic grant POSDRU ID77265 (2010), co-financed by the European Social Fund – Investing in People, within the Sectoral Operational Programme Human Resources Development 2007-2013. Dr. Sebastian Muntean was supported by Romanian Academy program.

## REFERENCES

1. Rusu O., Teodorescu M., Lascu-Simion N., *Material fatigue. Calculus guide*, 1, Ed. Tehnică, Bucharest, 1992. (in Romanian)
2. Bordeasu I., Popoviciu M., Marsavina L., Voda M., Negru R., Pirvulescu L., Numerical simulation of fatigue cracks initiation and propagation for horizontal axial turbines shafts, *Annals of DAAAM & Proceedings*, 407- 408, 2009.
3. Das G., Sinha A.N., Mishra S.K., Bhattacharya D., Failure analysis of counter shafts of a centrifugal pump, *Eng. Fail. Anal.*, 6:267-276, 1999.
4. Berndt F., van Bennekom A., Pump shaft failures - a compendium of case studies, *Eng. Fail. Anal.*, 8:135-144, 2001.
5. \*\*\* Alloy steels and high alloy steels for machine building, STAS 791-66, 1966 (in Romanian)
6. Davis J.R. (Editor), *ASM Specialty Handbook - Carbon and Alloy Steels*, ASM International, Metals Park, OH, 1996.

7. Liu Shu, Yuh J. Chao, Xiankui Zhu, Tensile-shear transition in mixed mode I/III fracture, *Int. J. of Solids and Struct.*, **41**:6147–6172, 2004.
8. Khoo S. W., Karuppanan S., Stress intensity factor for cracks emanating from a shaft, *J. of Appl. Science*, **11**(10):1839-1844, 2011.
9. Susmel L., *Multiaxial notch fatigue*, CRC Press, USA, 2009.
10. Unger D., *Analytical fracture mechanics*, Academic Press, USA, 1995.